Clinical Interventions in Aging

Dovepress
Taylor & Francis Group

Open Access Full Text Article

ORIGINAL RESEARCH

Causal Implication of CD52-Driven Immune Dysregulation in Sarcopenic Obesity: Integrating Mendelian Randomization and Multiomics Profiling

Saiyare Xuekelati[1], Yilihamu Abulitifu[2], Zhuoya Maimaitiwusiman[3], Lei Xu[1], Shuke Guo[1], Qihong Xu[1], Jiayu Ke[1], Hongmei Wang[3,4]

[1]Graduate School, Xinjiang Medical University, Urumqi, People's Republic of China; [2]Department of Infectious Diseases, People's Hospital of Xinjiang Uygur Autonomous Region, Urumqi, People's Republic of China; [3]Second Department of Comprehensive Internal Medicine, People's Hospital of Xinjiang Uygur Autonomous Region, Urumqi, People's Republic of China; [4]Xinjiang Medical University, Urumqi, People's Republic of China

Correspondence: Hongmei Wang, Email whmdoctor-xj@xjrmyy.com

Purpose: Sarcopenic obesity patients are likely to develop exacerbated metabolic dysfunction, while the mechanism linking sarcopenia and obesity is still unclear. This study aims to explore hub genes and immune-metabolic dysregulation related to the molecular pathogenesis of sarcopenia and obesity.

Methods: We used a public Gene Expression Omnibus (GEO) dataset to identify hub genes associated with sarcopenia and obesity. Weighted gene co-expression network analysis (WGCNA), protein-protein interaction (PPI), differentially expressed gene (DEG) analysis, GO/KEGG functional enrichment analyses and immune cell infiltration analysis were conducted to identify hub genes. Subsequently, these hub genes underwent multi-level validation.

Results: Integrated bioinformatics analysis identified 16 shared hub genes linked to the sarcopenia–obesity nexus. These genes were mainly enriched in immune-related pathways, as supported by immune infiltration profiling. External validation in independent cohorts confirmed CD52 as a common and central gene in both sarcopenia and obesity datasets, showing significant associations with immune cell characteristics. Mendelian randomization analysis indicated potential causal links between genetically predicted CD52 levels and reduced hand grip strength as well as increased body mass index, and these results were further supported by PCR assays in clinical samples.

Conclusion: The integrative analysis indicates that CD52 may function as a novel immunometabolic mediator in SO pathogenesis, underscoring its potential as a candidate biomarker for further study.

Keywords: Sarcopenia, obesity, bioinformatics, immune cell infiltration, Mendelian randomization

Introduction

As the global obesity epidemic converges with population aging, the complex interplay between excessive adiposity and progressive muscle decline has brought sarcopenic obesity (SO) to the forefront as a critical geriatric syndrome. SO, defined by the co-existence of sarcopenia and obesity, synergistically elevates the risk of mobility disability, metabolic diseases, and mortality, thereby imposing a substantial public health burden.[1,2] However, the reported incidence of SO exhibits substantial heterogeneity, with rates varying from 5.6% to as high as 66.6% across different populations and diagnostic criteria.[3–5] The 2025 updated Asian Working Group for Sarcopenia (AWGS) consensus reframes the condition by shifting the focus from disease management to lifelong muscle health promotion. It explicitly recognizes the critical cross-talk between muscle and adipose tissue, thus providing a compelling rationale for investigating sarcopenic obesity.[6] Given the increasing global incidence of SO, this elusive pathogenesis severely limits early intervention. Therefore, elucidating its core molecular mechanisms is a critical step toward alleviating the associated disease burden.

The pathogenesis of SO is driven by dysregulated crosstalk between adipose and muscle tissues, which is centrally mediated by chronic low-grade inflammation and concurrent hormonal alterations.[7] The expanded visceral adipose tissue

https://doi.org/10.2147/CIA.S570497
Received: 26 September 2025
Accepted: 16 January 2026
Published: 16 February 2026

in obese individuals acts as a prolific endocrine and immune organ. Critically, adipose tissue macrophages shift from an anti-inflammatory M2 phenotype to a pro-inflammatory M1 state, secreting a stream of pro-inflammatory cytokines—including interleukin-6 (IL-6), tumor necrosis factor-alpha (TNF-α), and interleukin-1 beta (IL-1β)—which spill over into the systemic circulation.[8,9] Our previous work, which demonstrated elevated plasma TNF-α levels in sarcopenia patients, provides direct clinical evidence linking such inflammatory pathways to muscle atrophy.[10] This inflammatory drive is further amplified by a concomitant disruption of the hormonal milieu that characterizes SO. In aging males, the obesity-associated shift from testosterone to estradiol contributes to a hypogonadal state that undermines muscle protein synthesis.[11] Similarly, in postmenopausal women, reduced estradiol and elevated FSH levels favor a shift in body composition toward adipose accumulation and muscle loss.[12] Furthermore, age- and obesity-related decreases in the levels of anabolic hormones such as growth hormone (GH) disrupt key muscle maintenance pathways.[13–15] Collectively, these adipose-driven inflammatory and hormonal alterations establish a state of systemic immunometabolic dysregulation that is central to SO pathogenesis.

These systemic immunometabolic signals destructively converge on skeletal muscle, establishing a direct "immune attack" on muscle integrity. The proinflammatory cytokines derived from adipose tissue, such as TNF-α and IL-6, act as primary effectors by activating the ubiquitin–proteasome and apoptotic pathways, leading to accelerated protein breakdown and cell death.[16] Concurrently, the ectopic lipid infiltration (myosteatosis) fueled by this inflammatory milieu introduces lipotoxicity, which impairs insulin signaling. The resulting insulin resistance serves as a critical amplifier, disrupting the anabolic mTORC1 pathway for protein synthesis[17–21] while activating the catabolic FoxO-mediated proteolytic system.[22,23] Thus, an immune-initiated cascade—from inflammatory signaling to metabolic dysfunction—orchestrates a self-perpetuating vicious cycle: muscle wasting begs further metabolic derangement and adipose tissue inflammation, which in turn exacerbates muscle loss. Despite this understanding of the effector pathways, the shared regulatory factors that initiate and coordinate immunometabolic crosstalk in SO remain unidentified, hindering a unified molecular understanding of this condition.

To identify these core regulatory factors and systematically decode the shared molecular architecture of SO, we implemented a hypothesis-driven, multi-omics strategy. We analyzed skeletal muscle transcriptomes from sarcopenia patients (GSE1428)[24] and adipose transcriptomes from obese patients (GSE2510)[25] to identify shared immune-related hub genes. The candidate genes subsequently underwent a multi-tier validation framework, including external transcriptomic verification, causal inference via Mendelian randomization (MR), and experimental confirmation in peripheral blood samples via quantitative reverse transcription PCR (qRT-PCR). This comprehensive strategy aims to decipher the core molecular architecture of SO and identify robust candidate targets for future mechanistic investigations.

Materials and Methods

Data Extraction

Matrix files and platform data for GSE1428 and GSE2510 were obtained from the National Center for Biotechnology Information Gene Expression Omnibus (NCBI-GEO) (https://www.ncbi.nlm.nih.gov/geo). The keywords "homo sapiens", "sarcopenia," and "obesity" were used to search for associated gene expression datasets: (1) each test sample was acquired from human tissue, and (2) the expression profiles in every dataset were independent. The exclusion criterion was participation in another clinical study for drugs or additional treatments. Ultimately, the series matrix files and platform information for GSE1428 and GSE2510 were downloaded. These two datasets were obtained using the Affymetrix Human Genome U133A Array platform (GPL96). GSE1428 included data from 12 older adults and 10 young individuals and covers the global gene expression profile of the vastus lateralis muscle.[26] GSE2510 included data from 14 obese patients and 14 normal individuals and focused on primary cultured abdominal subcutaneous preadipocytes.[27] In the validation section, we selected two datasets: GSE9103[28] and GSE151839.[29] GSE9103 used vastus lateralis muscle biopsy samples from 20 young adults and 20 young individuals, whereas GSE151839 used skin and fat biopsy samples from 20 individuals, including 10 obese and 10 normal-weight individuals. Both datasets were produced using the Affymetrix Human Genome U133 Plus 2.0 Array platform (GPL570). For the bioinformatic analyses utilizing public

data, no additional ethical approval was required, as all original studies providing the data had obtained the necessary approvals and participant consent.

Construction of Weighted Gene Co-Expression Network Analysis (WGCNA)

To identify gene co-expression modules associated with sarcopenia, we performed WGCNA on the GSE1428 dataset using the WGCNA R package.[30] First, pairwise genes were subjected to Pearson's correlation matrix and average linkage method analyses. Next, the power function A_mn =|C_mn|^β (C_mn = Pearson's correlation of Gene_m with Gene_n; A_mn = adjacency of Gene m with Gene n) was used to construct the weighted adjacency matrix. In the function, β represents the soft-thresholding parameter, probably emphasizing the potent gene relationships and penalizing weak correlations. When the power was selected to be 8, the adjacency was converted into the topological overlap matrix (TOM). The TOM can determine the network connectivity of one gene by the sum of adjacency with each other gene to generate a network, followed by the calculation of related dissimilarity (1-TOM). To classify genes that had close expression patterns in the gene modules, we conducted average linkage hierarchical clustering based on the TOM-based dissimilarity measure at a minimal size of 30 (gene group) for the gene dendrogram. We set the sensitivity at 3. For module analysis, the dissimilarity of module eigengenes was computed, the cutoff line was selected for the module dendrogram, and later, certain modules were pooled. Modules whose distances were less than 0.12 were merged, ultimately yielding four co-expression modules. The gray module was a collection of genes not assigned to one specific module. The correlations of the module feature vectors with gene expression were determined to obtain the MM. At the cutoff threshold (|MM| > 0.8), 905 highly connected genes from the clinically significant module were considered to be hub genes.

Differentially Expressed Gene (DEG) Screening

Differentially expressed genes (DEGs) were screened using the limma package of R (Version 4.5.1) in the obesity group versus the normal control group[31] based on the thresholds of |log FC|>1 and adjusted $P < 0.05$. Common DEGs were detected and visualized VennDiagram package.

Functional Annotation

Metascape (http://Metascape.org/gp/index.html) is a free web-based analytics tool for comprehensive gene annotation and analysis resources that combines GO and KEGG enrichment searches to leverage more than 40 independent knowledge bases.[32] To understand the roles of the DEGs and core genes, Metascape was used to conduct GO and KEGG analyses.

PPI Network Analysis

Search Tool for the Retrieval of Interacting Genes (STRING) (Version 11.3, https://cn.string-db.org/) is a web-based approach used to analyze protein interactions.[33] We mapped the DEGs and core genes to the STRING database and considered experimentally validated interactions whose combined scores were > 0.4 to be statistically significant. Later, the Cytoscape software (Version 3.5.1) (www.cytoscape.org/) was used to visualize the PPI network.[34] Hub genes were screened from the PPI network using the cytoHubba plug-in of Cytoscape. We selected the 10 genes with the greatest degree of significance as hub genes.[35]

Assessment of Immune Cell Infiltration by the MCP-Counter

We used a microenvironment cell population counter (MCP-counter) for assessing immune and stromal cell infiltration.[36] Next, the log2-transformed FPKM expression matrix after normalization was uploaded to the MCP-counter package (Version 1.1.0), which produced absolute abundance scores of the eight main types of immune cells (T cells, natural killer (NK) cells, cytotoxic lymphocytes, B lineage cells, myeloid dendritic cells, monocytic lineage cells, neutrophils, fibroblasts, and endothelial cells (ECs)). The deconvolution profiles were subsequently subjected to hierarchical clustering and comparison between sarcopenia patients and normal controls, and between obese patients and normal controls.

Additionally, Spearman correlation coefficients for the correlation between the hub genes and immune cells were determined.

Verification of Common Hub Genes via External Databases and ROC Evaluation

We further evaluated the prognostic value of the common hub genes by performing ROC analysis using the external datasets GSE9103 and GSE151839. We first validated the differential expression of candidate hub genes in two external databases by conducting non-parametric tests. Statistically significant genes, defined by $P < 0.05$, were subsequently subjected to ROC analysis in both external databases. Genes demonstrating an area under the curve (AUC) > 0.7 in the two cohorts were identified as the final common hub genes. Finally, we conducted a Pearson correlation analysis to assess the relationships of these validated hub genes with immune cell infiltration profiles.

Sources of Data for Mendelian Randomization Analysis

Through GWAS, complex disease-related genetic variants were identified by examining large populations of DNA samples; the findings revealed genes related to disease onset, progression, and treatment. In this study, we acquired eQTL data for CD52 (ENSEMBL ID: ENSG00000169442) from the eQTL catalog (https://www.ebi.ac.uk/eqtl/), which were derived from studies using peripheral blood as the source tissue. Single-nucleotide polymorphisms (SNPs) represent single-nucleotide variant-induced DNA sequence variations at the genome scale and account for more than 90% of identified polymorphisms. Detailed information on the datasets is presented in Table 1.

Mendelian Randomization Analysis

We used eQTL data for exposure, whereas sarcopenia and obesity GWAS data were used as the outcome for identifying genes related to sarcopenia and obesity; the analysis was performed in the R software (Version 4.5.1). SNPs closely related to sarcopenia or obesity were selected ($P < 5 \times 10^{-8}$). We later performed a clumping procedure ($r^2 < 0.01$ and clumping distance = 10,000 kb) to assess linkage disequilibrium (LD) among SNPs.[37] The beta coefficient of every allele, *p*-value, and standard error of every SNP were obtained from the sarcopenia and obesity GWAS dataset. Instrumental variables (IVs) significantly associated with the outcome phenotype were removed ($P < 5 \times 10^{-8}$). We then harmonized the SNP instruments by calibrating the directions of the alleles for both Exposure-SNPs and Outcome-SNPs and removing SNPs with ambiguous palindromic sequences. An F-statistic ($F = beta^2_{exposure}/SE^2_{exposure}$) >10 was selected as the threshold for reducing weak IV–induced bias.[38] Two-sample Mendelian randomization (MR) analysis was conducted using the "TwoSampleMR" package (Version 0.5.10). The primary analysis was performed using the inverse-variance weighted (IVW) method. To test the robustness of the findings, we additionally employed MR-Egger, weighted median, simple mode, and weighted mode methods. The significant deviation of the MR-Egger intercept from 0 was analyzed to examine horizontal pleiotropy. Horizontal pleiotropy was assessed using two approaches: (1) examining the significance of the MR-Egger regression intercept; and (2) applying the Mendelian Randomization Pleiotropy RESidual Sum and Outlier (MR-PRESSO) test to globally test for and correct for pleiotropy by identifying and removing outlier SNPs. Heterogeneity was detected with Cochran's Q statistic and associated p-values, with $P > 0.05$ indicating the absence of significant heterogeneity. Finally, leave-one-SNP-out analysis was performed to assess the reliability of the results and the possible influence of SNPs.

Table 1 GWAS Data Information on Sarcopenia and Obesity Related Traits

Outcome	ID.Outcome	Time	Number of SNPs	Sample size(n)	Population
Appendicular lean mass	ebi-a-GCST90000027	2020	18,164,071	244,730	European
Low hand grip strength	ebi-a-GCST90007528	2021	9,356,133	121,055	European
Usual walking pace	ukb-e-924_MID	2020	11,858,007	1521	Greater Middle Eastern
Body mass index	ebi-a-GCST90029007	2018	11,973,091	532,396	European

Abbreviation: SNPs, Single-nucleotide polymorphisms.

Participants

This cross-sectional study included community-dwelling elderly individuals from Xinjiang and was approved by the Ethics Committee of the People's Hospital of Xinjiang Uygur Autonomous Region (reference number: KY2021031726). Informed consent was obtained from all participants. For patients with language barriers or those who were illiterate, their legal guardians were coordinated, this questionnaire was translated into the local language, and their legal guardians provided informed consent. This study is registered with the Chinese Clinical Trial Registry (ChiCTR) at http://www.chictr.org.cn/ (registration number: ChiCTR2400093292).

The participants were derived from an epidemiological survey conducted in Mulei County, Xinjiang Uygur Autonomous Region, China, from June 20 to June 30, 2024. A two-stage random sampling method was used: first, 10 townships were randomly selected; second, about 100 adults aged ≥60 years were included per township. The participants underwent physical examinations, blood sampling, and a Comprehensive Geriatric Assessment (CGA), which included muscle strength evaluation, mobility assessments (assistance with walking, chair rising, and climbing stairs), and fall risk screening using the SARC-F questionnaire. Our inclusion criteria for the present epidemiological study were as follows: age ≥60 years, ability to ambulate independently without assistive devices, and provision of informed consent. The exclusion criteria were as follows: cognitive impairment, a history of psychiatric disorders, severe organ dysfunction (eg, cardiac/respiratory/renal/hepatic failure), recent surgical history (within three months), current use of corticosteroid medications, implanted electronic medical devices such as cardiac pacemakers, and active wasting diseases such as tuberculosis and cancer. A total of 1,316 participants were enrolled in this epidemiological study, and we excluded 42 individuals whose data were incomplete, leaving 1,274 eligible participants. Among them, 103 individuals were diagnosed with SO based on joint criteria.[39] As the diagnosis of SO varies by age, ethnicity, sex, and health status, with differing reference ranges for low muscle strength and low muscle mass, we established diagnostic criteria for Chinese older adults based on Asian population cohort studies and regional guidelines.[40] The SO diagnosis requires meeting all three criteria: screening positivity: (1) SARC-F score ≥4[41] plus obesity defined[42] as body mass index (BMI) ≥28 kg/m^2 or waist circumference (WC) ≥90 cm (male)/85 cm (female); (2) low muscle strength or function:[43] handgrip strength <28 kg (male) or <18 kg (female) and/or impaired physical performance (≥17 s on the five-time chair rise test); and low muscle mass: appendicular skeletal muscle mass adjusted for weight (SMM/W) <0.382 (men) or <0.322 (women).[44] Among the 103 individuals diagnosed with SO, only 16 provided consent to participate and usable serum samples. Non-SO controls (n = 1,171) were frequency-matched to SO cases by age (±3 years) and sex. The final inclusion criteria included the following blood samples: SO group: 16 patients whose serum samples were available; and control group: 18 matched non-SO individuals whose serum samples were available. Finally, 16 SO participants and 18 control participants were included to identify the hub genes associated with SO (Figure 1).

Throughout the interview, we recorded height, weight, BMI, WC, and handgrip strength when patients wore light indoor clothes and had no shoes. BMI was computed by dividing body weight (kg) by height (m^2).[45] The hand JAMAR dynamometer (JAMAR Hydraulic Hand Dynamometer, Lafayette, IN, USA) was used to measure handgrip strength, with the maximum reading of two trials being recorded.[46] Two readings were obtained from each side, and the maximum values of the right and left sides were used for the analysis. Weakness was defined as hand grip strength <28 kg for males and 18 kg for females. These parts are identical to those of our previous study.[47] Additionally, bioelectrical impedance analysis (BIA) was performed to assess skeletal muscle mass using an InBody S10 device (Biospace Co., Ltd., Seoul, Korea). Additionally, the history of major comorbidities—including hypertension, type 2 diabetes mellitus, myocardial infarction, and cerebrovascular disease—was systematically documented during the clinical assessment.

Sample Collection, RNA Extraction and Quantitative Reverse Transcription PCR (qRT-PCR) Assay

Venous blood samples were collected in EDTA tubes from SO patients (n=16) and non-SO controls (n=18) for qRT-PCR verification to confirm the results of bioinformatics analysis. Total RNA from peripheral blood was extracted using the RNA Isolation Reagent (Servicebio Technology Co., Wuhan, China) according to the manufacturer's instructions. The integrity of the total RNA was verified by 1.5% agarose gel electrophoresis, which confirmed the presence of intact 28S

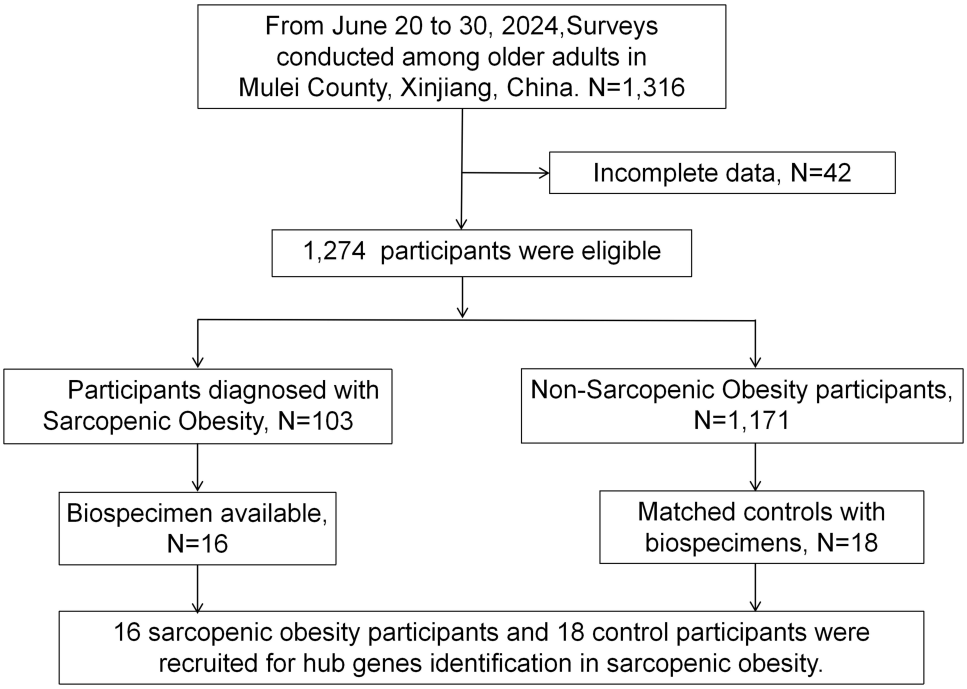

Figure 1 Selection procedure for the study participants.

and 18S rRNA bands in all the samples (Supplementary Figure S5). The concentration and purity (A260/A280 ratio between 1.8 and 2.2) of the extracted RNA were measured via a NanoDrop 2000 Spectrophotometer (Thermo Fisher Scientific). Subsequently, 200 ng of total RNA from each sample was reverse-transcribed into cDNA via the SweScript All-in-One RT SuperMix for qPCR (One-Step gDNA Remover) (Servicebio) following the kit protocol. This input amount falls within the kit's recommended range and was pre-validated in our pilot experiments to ensure efficient and stable cDNA synthesis. Next, qRT-PCR amplification was performed using a QuantStudio 6 Flex real-time fluorescent quantitative PCR system (Thermo Fisher Scientific, USA) with 2×Universal Blue SYBR Green qPCR Master Mix (Servicebio Technology Co., Wuhan, China). The $2^{-\Delta\Delta Ct}$ approach was adopted for quantifying mRNA expression, and β-actin was used as the normalization control for target gene expression. The primer sequences used included CD52 (forward: 5′- TCCTACTCACCATCAGCCTCC-3′, reverse: 5′- TGCCTCCGCTTATGTTGCT-3′), and β-actin (forward: 5′- CACCCAGCACAATGAAGATCAAGAT-3′, reverse: 5′-CCAGTTTTTAAATCCTGAGTCAAGC-3′).

Statistical Analysis

All statistical analyses were conducted using R (Version 4.5.1). The "TwoSampleMR" R package was used to perform two-sample MR analysis.[48] The inverse-variance weighted (IVW) method was employed as the primary analysis.[49] To test the robustness of the findings, we supplemented it with four additional MR methods: weighted median, MR-Egger, simple mode, and weighted mode. Horizontal pleiotropy was assessed using two complementary approaches: the MR-Egger intercept test[50] and the Mendelian Randomization Pleiotropy RESidual Sum and Outlier (MR-PRESSO) global test.[51] Heterogeneity across the genetic variant-specific estimates was evaluated using Cochran's Q statistic.[52] Furthermore, a leave-one-SNP-out analysis was conducted to examine if the overall results were driven by any single influential variant. An adjusted $P < 0.05$ (two-sided) indicated that the results were statistically significant.

Results

Bioinformatic Analysis Flowchart

The flowchart is presented in Figure 2 First, co-expression modules and key genes associated with sarcopenia were identified using WGCNA, and obesity-associated DEGs were detected with LIMMA. Functional enrichment analyses

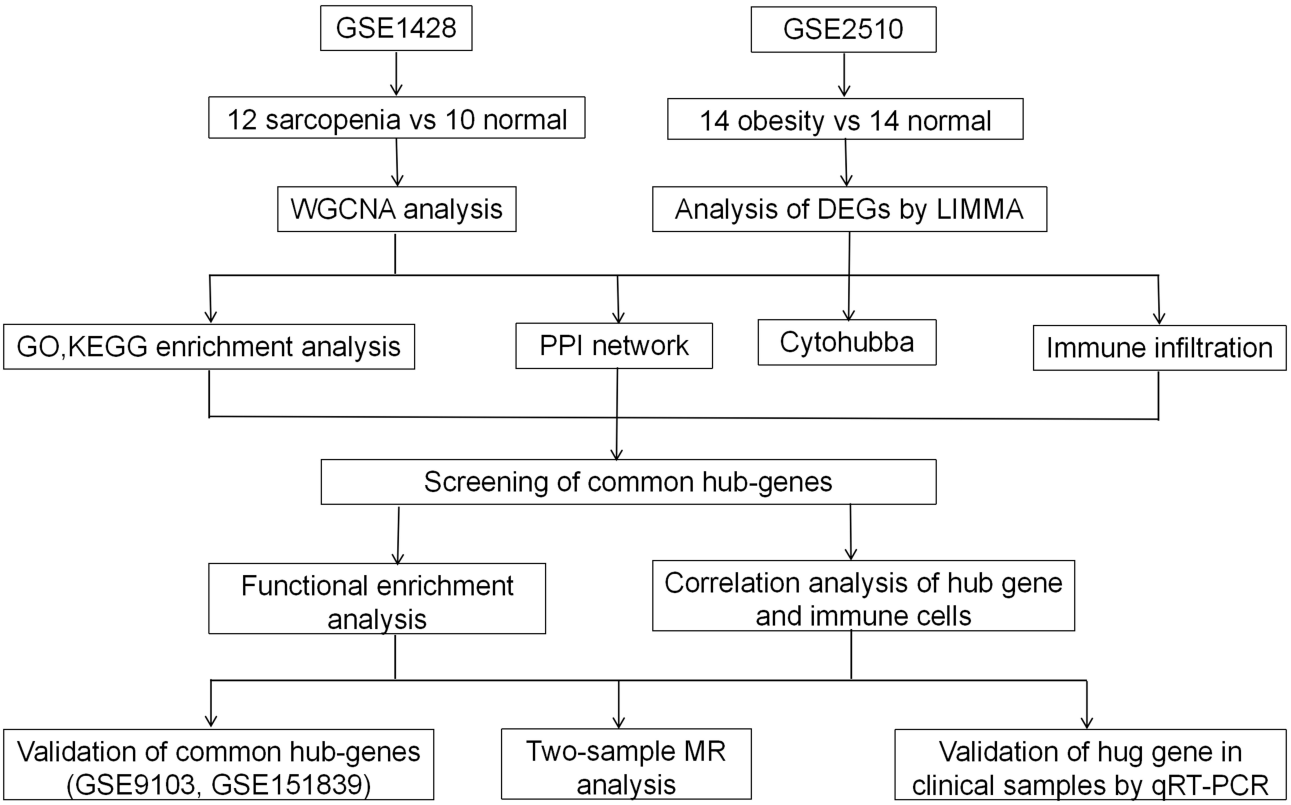

Figure 2 Flowchart of this study.
Abbreviations: GSE, Gene Expression Omnibus; WGCNA, Weighted Gene Co-expression Network Analysis; DEGs, Differentially Expressed Genes; LIMMA, Linear Models for Microarray and RNA-seq Data; GO, Gene Ontology; KEGG, Kyoto Encyclopedia of Genes and Genomes; PPI, Protein-Protein Interaction; qRT-PCR, Quantitative Real-Time PCR; MR, Mendelian Randomization.

(GO and KEGG) were conducted on WGCNA-derived key genes from sarcopenia patients and LIMMA-derived DEGs from obese patients. PPI network analysis was performed for significant gene sets obtained from both analyses, and hub genes within these networks were identified using CytoHubba. Concurrently, immune cell infiltration profiles were estimated for both datasets. Hub genes derived from sarcopenia, obesity, and shared PPI analyses were integrated to screen for common hub genes relevant to both conditions. These common hub genes were then rigorously validated using external datasets (GSE9103 and GSE151839) and clinical samples. Further characterization included functional annotation of the common hub genes, correlation analysis between hub gene expression and immune cell infiltration levels, and evaluation of diagnostic potential using ROC curves. MR analysis was conducted to assess potential causal relationships. Finally, molecular validation of the hub genes was performed by conducting qRT-PCR analysis.

Identification and Analysis of Hub Genes Associated with Sarcopenia by WGCNA

A scale-free co-expression network was established through WGCNA to identify the module most closely related to sarcopenia. We selected $\beta = 8$ (scale-free $R^2 = 0.95$) as the soft-thresholding power to ensure the scale-free network (Figure 3A and B). Four modules were obtained by conducting average linkage hierarchical analysis (Figure 3C and D). The MM of the black module ($r = 0.51$, $p = 0.01$) was closely related to the GS of sarcopenia, and the relationship of the MM with the GS of the black module was examined (Figure 3E). There were 4062 genes in the turquoise module, among which 905 were deemed core genes with high MM (>0.8) and GS (>0.1) values (Figure 3F). The main PPI network analysis of the 10 most significant hub genes was performed using the cytoHubba software, and the node color shading indicated the degree of connectivity (Figure 3G). As revealed by the results of the GO and KEGG analyses via the Metascape website, the core genes presented the greatest enrichment in immune system processes (Figure 3H).

https://doi.org/10.2147/CIA.S570497

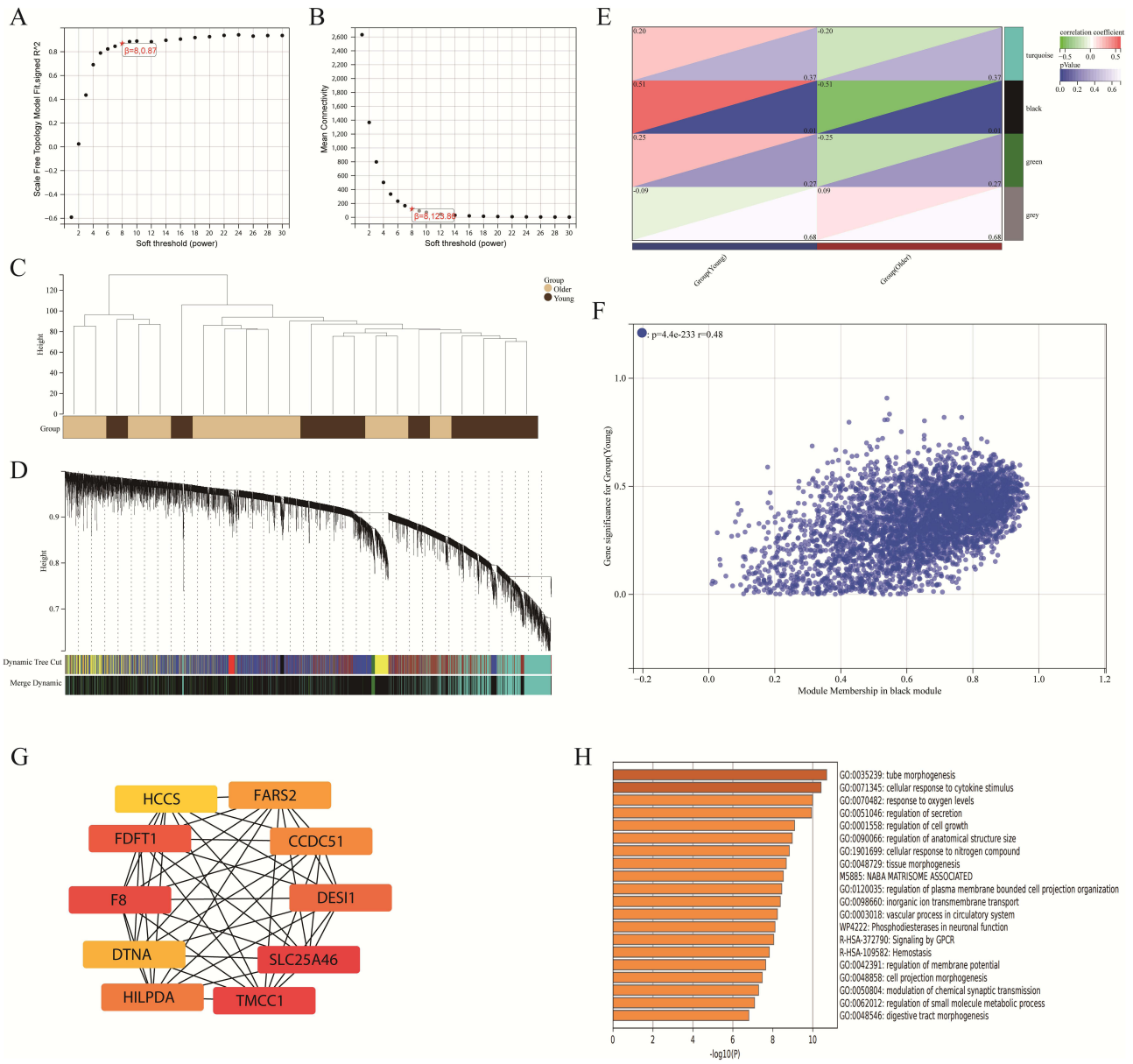

Figure 3 Screening of hub genes associated with sarcopenia. (**A** and **B**) Assessment of the scale-free fit index and the mean connectivity at different soft threshold clustering dendrograms of genes in the coexpression network. (**C** and **D**) Clustering dendrogram of differentially expressed genes (DEGs). (**E**) Correlation of modules and meta-module identification. (**F**) Scatter plot depicting the relationship between gene significance (GS) for sarcopenia and module membership (MM) in the black module (r=0.48, p=4.4e-233). Each dot indicates one gene in the module. The significant genes were filtered according to a GS >0.1 and MM >0.8. (**G**) Major PPI network analysis of the top 10 hub genes from 905 hub genes through cytoHubba software. (**H**) Functional annotation of the 905 hub genes involved in the black module.

Screening and Analysis of DEGs in the obesity Database

Using the limma package and thresholds of $|\log_2 FC| \geq 1.5$ and adj. $P < 0.05$, we identified 266 DEGs, with 171 upregulated genes and 95 downregulated genes. The volcano plot (Figure 4A) illustrates these DEGs in obese patients compared to controls. These 266 DEGs were uploaded to the STRING database to construct a PPI network. The heatmap clustering of DEGs between normal controls and obese patients is presented in Figure 4B. The cytoHubba plugin of Cytoscape was subsequently used to examine the hub genes with the "degree" algorithm. The genes CCR, CD86, FCGR2B, FCGR2A, PTPRC, TYROBP, CD74, SPI1, CTSS, and ITGB2 were the top 10 upregulated genes (Figure 4C), and the genes FGF8, KITLG, CXCL12, DKK1, KLF4, PTGS2, CD36, ITGA6, ENG, and ACAN were the top 10 downregulated genes (Figure 4D). GO and KEGG enrichment analyses of the above 20 hub genes were performed using

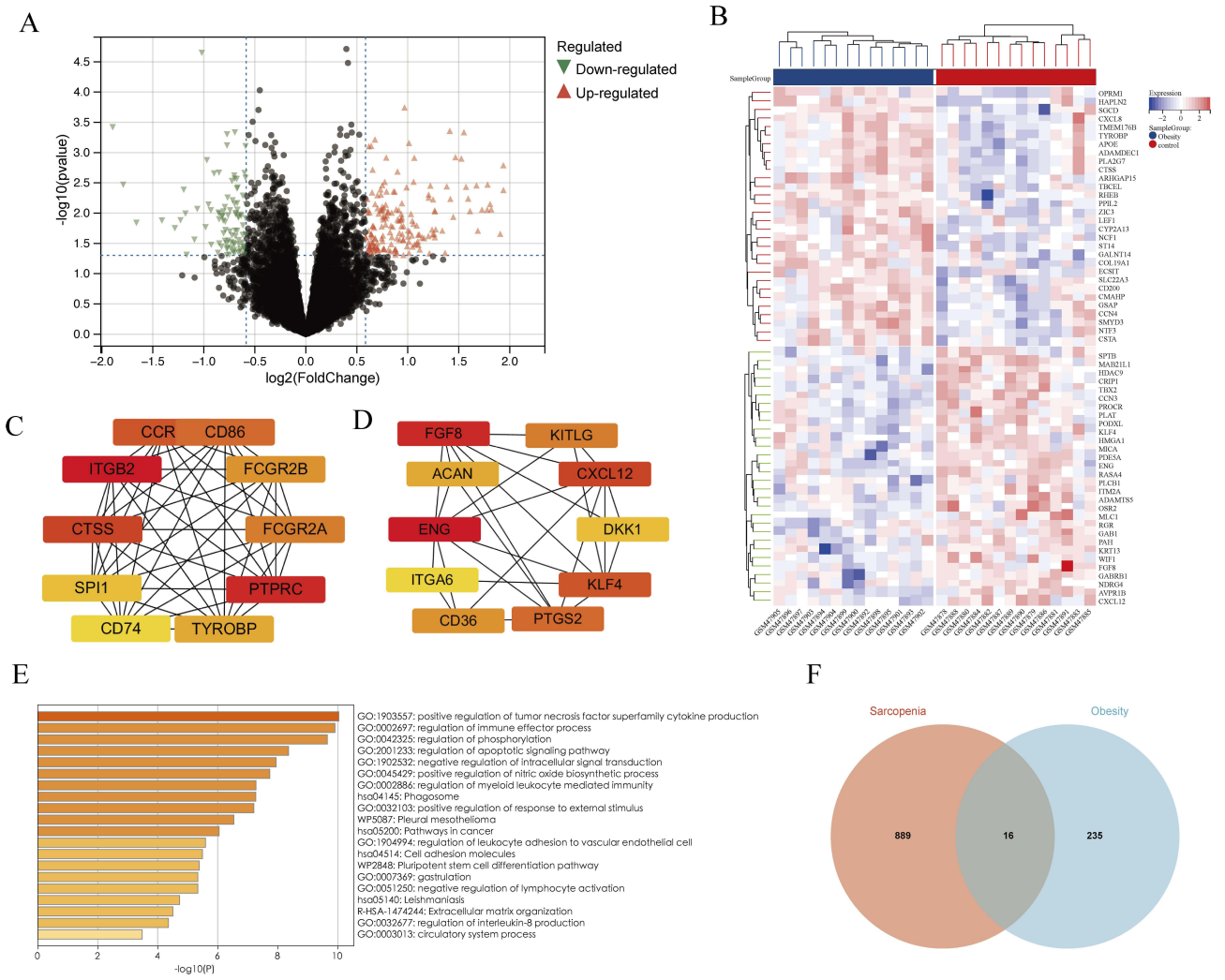

Figure 4 Screening of hub genes associated with obesity and Venn diagram of differentially expressed genes (DEGs) associated with obesity and sarcopenia. (**A**) Volcano plot of DEGs associated with obesity. (**B**) Heatmap clustering of the DEGs between normal controls and obese patients. (**C**) Major protein–protein interaction (PPI) network analysis of the top 10 hub genes among the upregulated genes. (**D**) Major PPI network analysis of the top 10 hub genes among the downregulated genes. (**E**) Functional annotation of the 20 hub genes contained in C and D. (**F**) Venn diagram showing the number of shared DEGs between obesity and sarcopenia.

Metascape (Figure 4E). The hub genes associated with sarcopenia were subsequently intersected with those associated with obesity using the Venn diagram package, and 16 shared DEGs were identified: ACAN, ADAMDEC1, AOC4P, CD52, CD53, CMAHP, COL19A1, CYP2C8, DCLRE1A, FGG, GABRB1, HDAC9, ITGA6, PLAC1, RPS6KA1, and TMEM140 (Figure 4F).

Immune Cell Infiltration and Immune Cell Correlation Analyses

To delineate the immunomodulatory effect of common hub genes, we profiled infiltrating immune cells, including T cells, cytotoxic lymphocytes, natural killer (NK) cells, B lineage cells, monocytic lineage cells, myeloid dendritic cells, neutrophils, ECs, and fibroblasts (Figure 5A and B), were analyzed with MCP-counter devolution. The violin plot showing immune cell infiltration differences revealed that the number of T cells, B cells, and NK cells was considerably lower in the sarcopenia group than in the control group. Additionally, the number of ECs was lower in both the sarcopenia and obesity groups than in the control group. The number of monocytic lineage cells, however, was greater in the obesity group than in the control group (Figure 5C and D). Next, Spearman correlation coefficients for the correlation between the hub genes and immune cell infiltration levels were determined. Consequently, T cells, B cells, ECs, and NK cells were positively associated with all 16 hub genes in the sarcopenia group. In the obesity cohort, ECs were positively

https://doi.org/10.2147/CIA.S570497

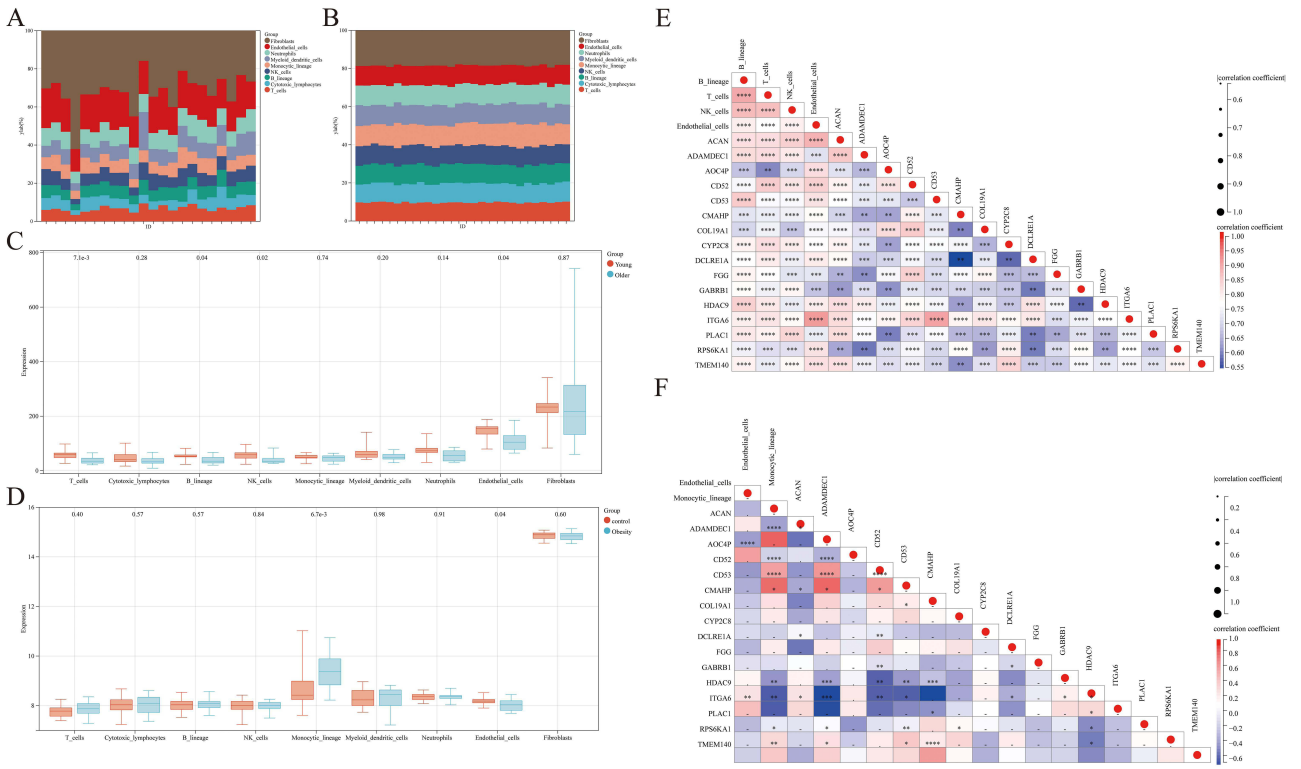

Figure 5 Immune cell infiltration analysis. (**A**) Heatmaps of the relative proportions of 9 infiltrating immune cells in patients with sarcopenia. (**B**) Heatmaps of the relative proportions of 9 infiltrated immune cells in patients with obesity. (**C**) Violin chart of the abundance of each type of immune cell infiltration in the sarcopenia and control groups. (**D**) Violin chart of the abundance of each type of immune cell infiltration in the obesity and control groups. (**E**) Correlation analysis of T lymphocytes (T cells), B lymphocytes (B cells), natural killer (NK) cells, endothelial cells (ECs) and hub genes in patients with sarcopenia. (**F**) Correlation analysis of ECs, monocytic lineages and hub genes in patients with obesity.

correlated with AOCP4 and ITGA6 expression. In contrast, monocytic lineage cells were positively correlated with ADAMDEC1, CD52, CD53, HDAC9, ITGA6, RPS6KA1, and TMEM140 expression (Figure 5E and F).

GO/KEGG–Functional Annotation of hub Genes

The results of the GO and KEGG analyses revealed the biological characteristics of the 16 overlapping DEGs. The enriched MFs were associated mainly with MHC class II receptor activity, peptide antigen binding, AMPA glutamate receptor activity, Notch binding, and sodium-dependent phosphate transmembrane transporter activity (Figure 6A). In the cellular component (CC) category, the DEGs were closely associated with vesicles, cytoskeletal parts, polymeric cytoskeletal fibers, and excitatory synapses (Figure 6B). Biological processes (BP) included animal organ development, tissue development, and epidermal cell differentiation (Figure 6C). Additionally, based on KEGG analysis, the above shared DEGs were mostly related to the cAMP pathway, cell adhesion molecules (CAMs), and graft-versus-host disease (Figure 6D). The Human Reference Protein Interactome Mapping Project was adopted for visualizing the PPI network for intersecting DEGs between sarcopenia and obesity, and the confidence score was > 0.6, with 141 interaction pairs included (Figure 6E). Collectively, integrated GO and KEGG analyses demonstrated that SO orchestrates pathological crosstalk between immune dysregulation and metabolic reprogramming, driving tissue degeneration in muscle and adipose compartments.

Validation and Prediction of Hub Genes in the GEO Database

To validate the hub gene levels in skeletal muscle tissue and adipose tissue, we selected the GSE9103 and GSE151839 datasets as the validation datasets. As shown in Figure 7A and B, CD52, CMAHP, and ITGA6 levels were markedly lower in the skeletal muscle tissue of sarcopenia patients than in that of normal controls. In contrast, ADAMDEC1,

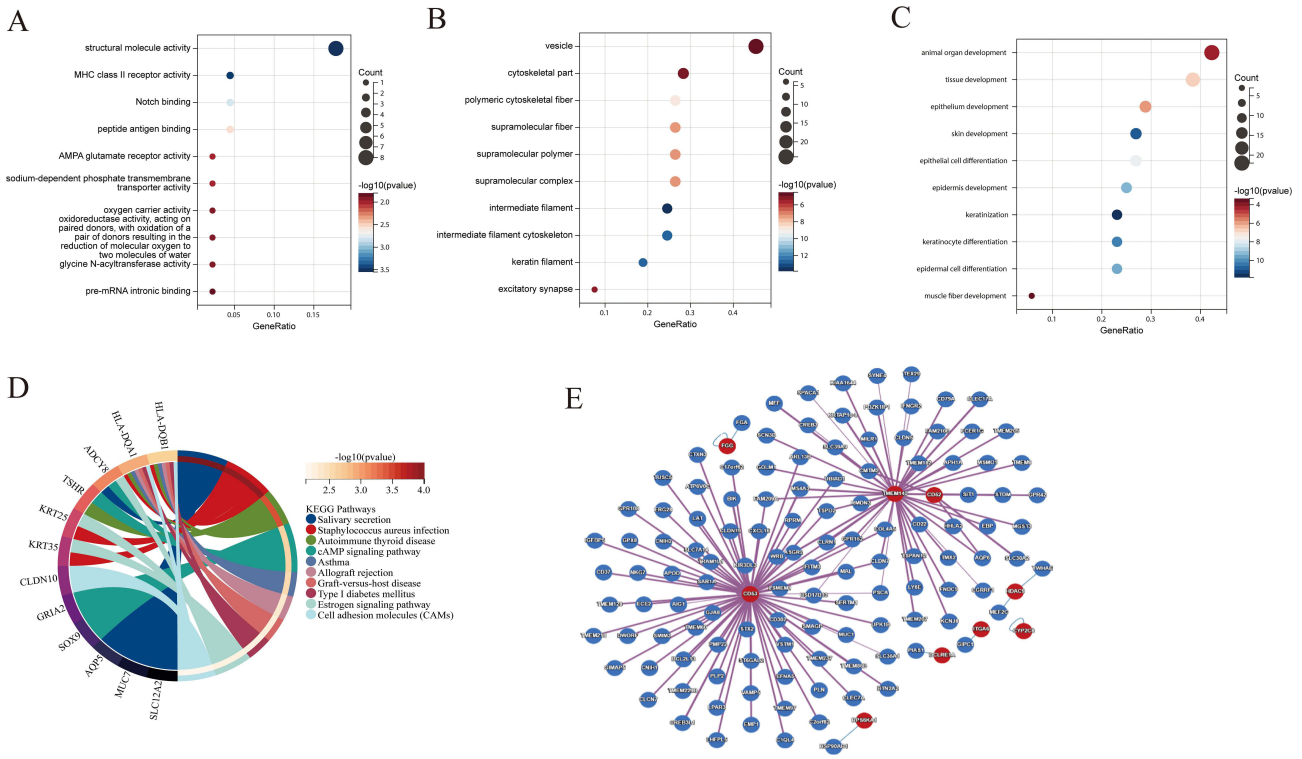

Figure 6 Functional analysis of the identified common differentially expressed genes (DEGs). (**A**–**C**) Gene Ontology (GO) enrichment analysis (molecular function (MF), cellular component (CC) and biological process (BP)). (**D**) Kyoto Encyclopedia of Genes and Genomes (KEGG) pathway analysis. (**E**) Protein–protein interaction (PPI) network of overlapping DEGs in sarcopenia and obesity via the Human Reference Protein Interactome Mapping Project (Query-Interactor). The red circles represent the hub genes.

CD52, and CD53 expressions were considerably higher in the adipose tissue of obese individuals than in the adipose tissue of controls. However, HDAC9 expression was significantly lower in the obese adipose tissue group. We performed ROC analyses on the genes with significant differences in gene expression in the external dataset validation. For obesity, the AUC of CD52 was 0.68 (0.50–0.86), that of ADAMDEC1 was 0.71 (0.53–0.88), that of CD53 was 0.79 (0.64–0.95), and that of HDAC9 was 0.71 (0.55–0.88) (Figure 7C–F). For sarcopenia in the external dataset, the AUC of CD52 was 0.75 (0.58–0.91), that of CMAHP was 0.69 (0.51–0.87), and that of ITGA6 was 0.69 (0.50–0.87) (Figure 7G–I). Based on these results, CD52 was identified as the only gene with significant differences in expression and good diagnostic performance in both external datasets. These results increase the reliability and consistency of the hub gene expression patterns across multiple datasets, which support their effects on the pathogenic mechanisms of sarcopenia and obesity. We subsequently conducted Spearman correlation analyses between CD52- and sarcopenia-associated immune cells and between CD52- and obesity-associated immune cells. The results revealed that CD52 was correlated with all nine sarcopenia-related immune cell types (Figure 7K); moreover, it was significantly correlated with monocytic lineage cells, an obesity-related immune cell type (Figure 7L).

Associations of CD52 with Sarcopenia and Obesity

We conducted MR analysis to estimate the causal effect size of the CD52 level on sarcopenia obesity. Using the primary IVW method, genetically predicted higher circulating CD52 levels were significantly associated with lower hand grip strength (β_IVW = –0.054, 95% CI: –0.091 to –0.017, $P = 0.004$) and higher BMI (β_IVW = 0.010, 95% CI: 0.004 to 0.015, $P < 0.001$) (Table 2). The robustness of these causal inferences was supported by a suite of sensitivity analyses. The associations of genetically predicted CD52 with low hand grip strength, usual walking pace, and body mass index (BMI) showed no evidence of horizontal pleiotropy (MR-Egger intercept $P = 0.086$, 0.270, and 0.615, respectively) or significant heterogeneity (IVW Q P-value = 0.923, 0.624, and 0.762, respectively). The MR-PRESSO global test

https://doi.org/10.2147/CIA.S570497

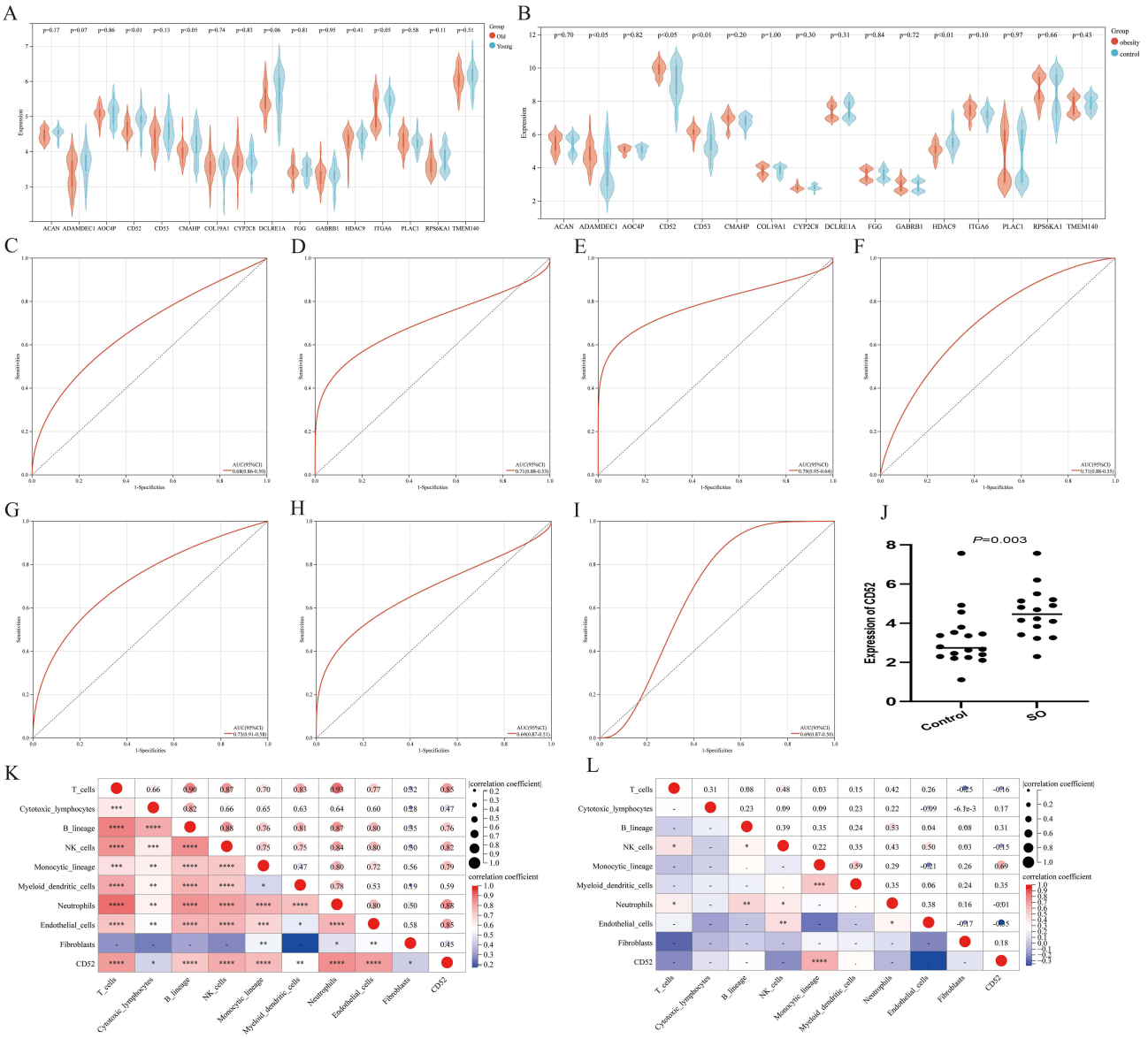

Figure 7 Validation of the hub genes in the external datasets. (**A**) Validation of the hub genes associated with sarcopenia in GSE9103. (**B**) Validation of the hub genes associated with obesity in GSE151839. (**C**–**F**) AUC of CD52, ADAMDEC1, CD53, and HDAC9 in GSE151839. (**G**–**I**) AUC of CD52, CMAHP and ITGA6 in GSE9103. (**J**) The expression levels of CD52 in sarcopenic obesity (SO) patients determined via quantitative real-time PCR (qRT–PCR). (**K**) Correlation analysis of CD52+ and 9+ infiltrating immune cells in GSE1428. (**L**) Correlation analysis of CD52+ and 9+ infiltrating immune cells in the GSE2510 dataset.
Note: ****$P < 0.0001$, ***$P < 0.001$, **$P < 0.01$, *$P < 0.05$.

confirmed the absence of distorting outliers for these traits (P = 0.927, 0.963, and 0.776, respectively) (Table 3). In contrast, the result for appendicular lean mass requires caution. The significant heterogeneity (IVW Q P-value < 0.001) and significant MR-PRESSO global test (P < 0.001) suggest that the genetic instruments may influence lean mass through multiple pathways beyond CD52. Although the MR-Egger intercept test did not indicate directional pleiotropy (P = 0.202), the presence of significant heterogeneity necessitates a cautious interpretation of the causal estimate for this specific outcome. (The detailed results of the Mendelian randomization analyses are presented in Supplementary Figures S1–S4).

Molecular Verification of Hub Genes by qRT-PCR

We conducted qRT-PCR to validate the hub gene levels in sarcopenic and obese synovial tissue. The baseline characteristics and CD52 expression levels in the SO and normal control groups are shown in Table 4. We included

Table 2 Mendelian Randomization Analysis of CD52 on the Risk of Sarcopenia and Obesity

Outcome	GWAS ID	n.SNP	Method	Beta(95% CI)	Estimates	*P*-value
Appendicular lean mass	ebi-a-GCST90000027	26	IVW	−0.001(−0.014~0.011)	0.006	0.837
			Weighted median	0.01(−0.003~0.023)	0.006	0.118
			MR Egger	0.022(−0.015~0.059)	0.019	0.255
			Simple mode	0.015(−0.011~0.042)	0.014	0.266
			Weighted mode	0.012(−0.001~0.025)	0.007	0.072
Low hand grip strength	ebi-a-GCST90007528	29	IVW	−0.054(−0.091~-0.017)	0.019	0.004**
			Weighted median	−0.04(−0.094~0.015)	0.028	0.157
			MR Egger	0.038(−0.07~0.146)	0.055	0.493
			Simple mode	−0.111(−0.207~-0.015)	0.049	0.032*
			Weighted mode	−0.02(−0.081~0.041)	0.031	0.534
Usual walking pace	ukb-e-924_MID	29	IVW	−0.003(−0.007~0.001)	0.002	0.196
			Weighted median	−0.005(−0.011~0.002)	0.003	0.153
			MR Egger	0.004(−0.008~0.016)	0.006	0.544
			Simple mode	−0.008(−0.019~0.003)	0.006	0.166
			Weighted mode	−0.006(−0.014~0.002)	0.004	0.147
Body mass index	ebi-a-GCST90029007	30	IVW	0.01(0.004~0.015)	0.003	<0.001***
			Weighted median	0.009(0.001~0.017)	0.004	0.029*
			MR Egger	0.006(−0.01~0.022)	0.008	0.473
			Simple mode	0.01(−0.004~0.023)	0.007	0.165
			Weighted mode	0.008(0~0.017)	0.004	0.066

Note: ***$P < 0.001$, **$P < 0.01$, *$P < 0.05$.
Abbreviations: IVW, Inverse-variance weighted; SNP, Single nucleotide polymorphism.

Table 3 Assessment of Pleiotropy and Heterogeneity in the Mendelian Randomization Analysis of CD52 and Sarcopenic Obesity

Outcome	Pleiotropy Test (MR-Egger Intercept *P*-value)	Heterogeneity Test (IVW Q *P*-value)	MR-PRESSO Global *P*-value
Appendicular lean mass	0.202	<0.001***	<0.001***
Low hand grip strength	0.086	0.923	0.927
Usual walking pace	0.270	0.624	0.963
Body mass index	0.615	0.762	0.776

Note: ***$P < 0.001$.
Abbreviations: IVW, Inverse-variance weighted; MR-PRESSO, Mendelian Randomization Pleiotropy RESidual Sum and Outlier.

34 participants in this study, with 18 individuals in the control group and 16 individuals in the SO group. The SO group presented significantly greater TP levels (75.0 vs 71.1, $P = 0.012$). No significant differences in age, gender, electrolytes (including Na), liver/kidney markers (TBIL, DBIL, GGT, BUN, and UA), CK levels or the prevalence of major cardiometabolic comorbidities (hypertension, type 2 diabetes, myocardial infarction, or cerebrovascular disease) between

the two groups (all $P > 0.05$; Table 4). Critically, CD52 expression was significantly greater in the SO group than in the control group (Figure 7J, Table 4), suggesting its potential role as a hub gene in SO pathogenesis.

Table 4 Baseline Characteristics of the Study Participants

Variables	Total (n = 34)	Non-Sarcopenic Obesity (n = 18)	Sarcopenic Obesity (n = 16)	Statistic	*P*
Gender, n(%)				-	0.693
Men	8 (23.529)	5 (27.778)	3 (18.750)		
Women	26 (76.471)	13 (72.222)	13 (81.250)		
Age, Mean ± SD	71.176 ± 6.417	70.833 ± 6.271	71.562 ± 6.762	t=−0.326	0.746
TBIL, Mean ± SD	11.901 ± 6.667	10.266 ± 4.316	13.741 ± 8.357	t=−1.549	0.131
DBIL, Mean ± SD	4.343 ± 1.951	4.150 ± 1.402	4.559 ± 2.459	t=−0.586	0.563
TP, Mean ± SD	72.924 ± 4.683	71.079 ± 3.775	75.000 ± 4.839	t=−2.649	0.012*
GGT, Mean ± SD	27.029 ± 15.458	28.389 ± 20.027	25.500 ± 8.149	t=0.562	0.580
BUN, Mean ± SD	6.936 ± 2.585	7.236 ± 2.077	6.599 ± 3.095	t=0.712	0.481
UA, Mean ± SD	295.588 ± 80.115	292.333 ± 79.131	299.250 ± 83.647	t=−0.248	0.806
K^+, Mean ± SD	4.274 ± 0.483	4.310 ± 0.431	4.234 ± 0.548	t=0.450	0.656
Cl^-, Mean ± SD	108.082 ± 3.252	108.030 ± 2.820	108.140 ± 3.774	t=−0.097	0.923
Ca^{2+}, Mean ± SD	2.356 ± 0.100	2.366 ± 0.105	2.346 ± 0.096	t=0.576	0.569
P, Mean ± SD	1.095 ± 0.219	1.101 ± 0.252	1.088 ± 0.183	t=0.170	0.866
Mg^{2+}, Mean ± SD	0.956 ± 0.057	0.961 ± 0.060	0.951 ± 0.055	t=0.503	0.618
CK, M (Q_1, Q_3)	83.470 (68.468, 115.775)	88.030 (73.988, 115.775)	81.005 (58.240, 97.745)	Z=−0.871	0.384
Na^+, M (Q_1, Q_3)	145.030 (143.555, 146.207)	145.210 (144.597, 145.990)	144.680 (143.462, 146.468)	Z=−0.289	0.772
CD52, M (Q_1, Q_3)	3.49 (2.58, 4.83)	2.74 (2.29, 3.60)	4.46 (3.52, 5.18)	Z=−2.968	0.003**
Myocardial infarction, n (%)				-	0.094
No	31 (91.18)	18 (100.00)	13 (81.25)		
Yes	3 (8.82)	0 (0.00)	3 (18.75)		
Cerebrovascular disease, n (%)				-	0.214
No	27 (79.41)	16 (88.89)	11 (68.75)		
Yes	7 (20.59)	2 (11.11)	5 (31.25)		
Type 2 diabetes mellitus, n (%)				-	0.164
No	29 (85.29)	17 (94.44)	12 (75.00)		
Yes	5 (14.71)	1 (5.56)	4 (25.00)		
Hypertension, n(%)				-	0.738
No	14 (41.18)	8 (44.44)	6 (37.50)		
Yes	20 (58.82)	10 (55.56)	10 (62.50)		

Note: $^{**}P < 0.01$, $^{*}P < 0.05$.

Abbreviations: TBIL, Total Bilirubin; DBIL, Direct Bilirubin; TP, Total Protein; GGT, Gamma-Glutamyl Transferase; BUN, Blood Urea Nitrogen; UA, Uric Acid; K^+, Serum Potassium; Cl^-, Serum Chloride; Ca^{2+}, Serum Calcium; P, Serum Phosphorus; Mg^{2+}, Serum Magnesium; CK, Creatine Kinase; Na^+, Serum Sodium; *t*, *t*-test; Z, Mann–Whitney test; -, Fisher exact; SD, standard deviation; M, Median; Q_1, 1st Quartile; Q_3, 3st Quartile.

Discussion

SO represents a complex clinical syndrome where the degenerative process of sarcopenia and the metabolic dysregulation of obesity converge, yet the shared molecular mechanisms remain poorly defined. Our integrated bioinformatics analysis directly addressed this gap by identifying 16 common hub genes (ACAN, ADAMDEC1, AOC4P, CD52, CD53, CMAHP, COL19A1, CYP2C8, DCLRE1A, FGG, GABRB1, HDAC9, ITGA6, PLAC1, RPS6KA1, and TMEM140) that functionally bridge these two conditions, with functional enrichment pointing overwhelmingly to immune-metabolic dysregulation as a central pathogenic axis. Among these, the glycoprotein CD52 emerges as a pivotal immunometabolic mediator. Expressed on immune cells, CD52 is directly implicated in lipid-driven inflammation, with documented overexpression in oxidized LDL-induced foam cells and unstable carotid plaques. This finding provides a plausible mechanistic link between adipose tissue expansion and the chronic inflammatory state characteristic of SO.[53,54] This immune dysregulation is further coordinated by other hub genes: CD53, which modulates innate immunity and MHC class II activity, [55–57] and PLAC1, which may promote fibrotic remodeling.[58] Concurrently, metabolic reprogramming is driven by genes such as CYP2C8[59] and RPS6KA1, which exhibit a dual role in suppressing adipogenesis via STAT3-mediated degradation of KLF3[60] while potentially promoting lipid accumulation via cAMP signaling.[61] Together, these dysregulated pathways establish a vicious cycle of immune-metabolic dysfunction, thereby driving the progression of SO.

Our multi-omics integration delineates a new paradigm for SO pathogenesis, positioning it as a state of divergent yet complementary immune dysregulation between muscle and adipose tissues. This "see-saw" pattern reflects a paradoxical coexistence of immune impoverishment in sarcopenic muscle and inflammatory overactivation in obese adipose tissue. Specifically, we observed a marked depletion of adaptive immune cells—including T cells, B cells, and NK cells—in skeletal muscle, a result consistent with established clinical reports of impaired T-cell infiltration,[62] and further supported by correlations with the identified hub genes.[63,64] These findings suggest that insufficient immune surveillance and response, rather than inflammation alone, may contribute to progressive muscle wasting. In contrast, the obese microenvironment was dominated by innate immune hyperactivity, shown by the expansion of monocytic lineage cells and the upregulation of pro-inflammatory pathways such as neutrophil extracellular trap formation.[65] A key and unifying observation from our study is that these opposing immunological states converge on a shared pathophysiological event: the widespread depletion of ECs. Given the well-established role of skeletal muscle ECs as a major source of pro-regenerative factors such as brain-derived neurotrophic factor (BDNF),[66–68] their loss in both conditions is unlikely to be incidental. We propose that EC depletion acts as a final common pathway, linking adaptive immune failure in muscle to innate inflammatory activation in obesity, thereby creating a self-perpetuating cycle that drives SO progression.[69] Taken together, our data support an integrated, systems-level view of SO pathogenesis. Within this framework, CD52 emerges as a molecular candidate implicated in the related inflammatory and metabolic processes.

We therefore investigated CD52's potential role as a molecular driver. Although well recognized as a lymphocyte surface marker,[70] our data implicate CD52 in lipid-driven inflammation[53,71] and adipose tissue remodeling via the TGF-β/Smad3 pathway.[72] Its influence may further extend to skeletal muscle. Functional enrichment analysis revealed a significant clustering of SO-associated genes around MHC class II receptor activity.[73] Given the observed association between CD52 and monocytic-lineage cells—which serve as key MHC II expressers—it is plausible that CD52 modulates antigen presentation, potentially leading to aberrant CD4+ T-cell activation. This idea is compelling in the context of immunosenescence, where expansion of pathogenic CD4+CD28null T cells has been linked to muscle atrophy.[74] Moreover, efficient muscle regeneration depends on finely tuned immune-muscular crosstalk.[75,76] CD52 dysregulation could therefore impair this essential crosstalk. Thus, we propose a unifying model wherein CD52 sits at the nexus of a self-reinforcing pathogenic cycle: in obese adipose tissue, it fuels meta-inflammation and insulin resistance; concurrently, in aged muscle, it may disrupt the immunoregulatory balance required for repair, collectively accelerating tissue degeneration in SO.

To establish causal relationships, we implemented MR analysis. This approach showed that genetically predicted elevation of CD52 was positively associated with obesity risk and inversely associated with grip strength, providing strong genetic evidence that CD52 is a causal driver of the metabolic–muscular imbalance central to SO. These genetic

findings were further supported by our clinical validation, which demonstrated significantly higher levels of CD52 in the peripheral blood of SO patients. This observation extends the pathological relevance of CD52 beyond individual tissues and suggests its involvement as a systemic mediator in SO-related crosstalk. The rise in circulating CD52 is consistent with an expanding body of evidence on its immunometabolic functions. Notably, this aligns with a mechanism described in type 2 diabetes (T2DM), where increased soluble CD52 promotes a shift toward pro-inflammatory $CD4^{+}CD52$^high T cells, thereby worsening insulin resistance.[72] Given the shared features of chronic inflammation and impaired insulin regulation in both T2DM and SO, a similar pattern of CD52-mediated T-cell polarization may occur in SO, potentially disturbing muscle homeostasis through paracrine signals from inflamed adipose tissue. In summary, by integrating genetic causality with clinical profiling, this study supports CD52 as a key regulatory node connecting systemic immune dysregulation to the combined metabolic and muscular decline observed in SO. Future work should focus on assessing CD52-driven immune cell infiltration in skeletal muscle and characterizing CD52-high T-cell subsets in SO to clarify their precise mechanistic roles.

In summary, this study establishes an integrated multi-omics framework that moves beyond single-disease approaches to clarify the shared molecular pathogenesis of SO. By systematically cross-analyzing molecular networks from sarcopenia and obesity, key hub genes relevant to SO were identified, overcoming limitations inherent in studying each condition independently. The biological and clinical significance of these findings was supported through multiple layers of validation, including independent transcriptional datasets, clinical specimens, Mendelian randomization, and immune infiltration analyses. While the study provides substantial insights, several limitations should be acknowledged. First, the foundational transcriptomic datasets (eg, GSE1428, 2004) were generated prior to the establishment of contemporary diagnostic criteria for sarcopenia; nevertheless, the original studies were phenotypically rigorous, and our multilevel validation across independent cohorts supports the robustness of the identified signals. Second, our analyses integrated data from populations of distinct ancestries (European, American, and Asian). Although this limits direct cross-population generalizability, the consistency of the CD52 signal across these analytical stages provides initial evidence for its conserved role. Further validation in large, multi-ancestry cohorts is warranted. Third, although CD52 shows promise as a biomarker, it should be viewed as a complementary tool for risk stratification or early screening rather than a replacement for gold-standard diagnostic methods such as DXA or BIA. Finally, the modest size of our clinical cohort underscores the need for larger, multi-center studies to increase the generalizability of our conclusions. Furthermore, the study is based on computational and clinical human data; thus, the precise mechanistic role of CD52 awaits experimental validation in animal or cellular models of SO. We propose several prioritized research directions. Future studies should aim to (1) validate these findings in large, multi-ancestry prospective cohorts; (2) employ single-nucleus and spatial transcriptomics to deconvolute cell type-specific interactions; and (3) utilize experimental modulation of CD52 in model systems to definitively establish its functional role. Overall, this work provides initial evidence and lays the groundwork for a refined mechanistic understanding of SO, positioning CD52 as a candidate biomarker and a compelling focus for future investigations.

Conclusion

In conclusion, integrating network biology, genetic epidemiology, and clinical validation identifies CD52 as a potential immunometabolic hub in SO. The genetic analyses offer new evidence for a causal association between elevated CD52 and both increased BMI and reduced handgrip strength, indicating a connection between adiposity and muscle impairment. These results suggest CD52 as a candidate biomarker and advance understanding of SO as a condition shaped by immune–metabolic interactions, providing direction for future studies on its specific biological roles.

Data Sharing Statement

The publicly available data used in this study are detailed in the Methods section, including: Transcriptomic data from the Gene Expression Omnibus (GEO) database. Genetic association data from the OpenGWAS database and the eQTL Catalog. The individual-level data from our epidemiological cohort and the raw PCR validation data are not publicly available due to privacy and ethical restrictions but are available from the corresponding author upon reasonable request, subject to a formal data sharing agreement and approval from our institutional ethics committee.

Ethics Approval and Consent to Participate

The study was conducted according to the guidelines of the Declaration of Helsinki, and approved by Ethics Committee of the People's Hospital of Xinjiang Uygur Autonomous Region (approval number: KY2021031726). All participants provided written informed consent for participation and data collection.

Consent for Publication

The informed consent was voluntarily signed by the participants.

Acknowledgments

We would like to express our sincere gratitude to the director of Public Health Bureau for their continuous support of our population survey in the Mulei. We thank all the staff of the Second Department of Comprehensive Internal Medicine of People's Hospital of Xinjiang Uygur Autonomous Region, for their support with data collection.

Funding

The study was supported by the National Natural Science Foundation of China (82160276) and "Tianshan Talent" High-Level Medical and Health Talents Training Program (TSYC202301A004).

Disclosure

The author reports no conflicts of interest in this work.

References

1. Poggiogalle E, Lubrano C, Sergi G, et al. Sarcopenic obesity and metabolic syndrome in adult caucasian subjects. *J Nutr Health Aging*. 2016;20(9):958–963. doi:10.1007/s12603-015-0638-1
2. Chuan F, Chen S, Ye X, et al. Sarcopenic obesity predicts negative health outcomes among older patients with type 2 diabetes: the ageing and body composition of diabetes (ABCD) cohort study. *Clin Nutr*. 2022;41(12):2740–2748. doi:10.1016/j.clnu.2022.10.023
3. Murdock DJ, Wu N, Grimsby JS, et al. The prevalence of low muscle mass associated with obesity in the USA. *Skeletal Muscle*. 2022;12(1):26. doi:10.1186/s13395-022-00309-5
4. Yu B, Jia S, Sun T, et al. Sarcopenic obesity is associated with cardiometabolic multimorbidity in Chinese middle-aged and older adults: a cross-sectional and longitudinal study. *J Nutr Health Aging*. 2024;28(10):100353. doi:10.1016/j.jnha.2024.100353
5. Kim TN, Yang SJ, Yoo HJ, et al. Prevalence of sarcopenia and sarcopenic obesity in Korean adults: the Korean sarcopenic obesity study. *Int J Obes*. 2009;33(8):885–892. doi:10.1038/ijo.2009.130
6. Chen LK, Hsiao FY, Akishita M, et al. A focus shift from sarcopenia to muscle health in the Asian working group for Sarcopenia 2025 consensus update. *Nat Aging*. 2025;5(11):2164–2175. doi:10.1038/s43587-025-01004-y
7. Wei S, Nguyen TT, Zhang Y, Ryu D, Gariani K. Sarcopenic obesity: epidemiology, pathophysiology, cardiovascular disease, mortality, and management. *Front Endocrinol*. 2023;14:1185221. doi:10.3389/fendo.2023.1185221
8. Olefsky JM, Glass CK. Macrophages, inflammation, and insulin resistance. *Annu Rev Physiol*. 2010;72(1):219–246. doi:10.1146/annurev-physiol-021909-135846
9. Nunan E, Wright CL, Semola OA, et al. Obesity as a premature aging phenotype — implications for sarcopenic obesity. *Geroscience*. 2022;44(3):1393–1405. doi:10.1007/s11357-022-00567-7
10. Xuekelati S, Maimaitiwusiman Z, Bai X, Xiang H, Li Y, Wang H. Sarcopenia is associated with hypomethylation of TWEAK and increased plasma levels of TWEAK and its downstream inflammatory factor TNF-α in older adults: a case-control study. *Exp Gerontol*. 2024;188:112390. doi:10.1016/j.exger.2024.112390
11. Shin MJ, Jeon YK, Kim IJ. Testosterone and Sarcopenia. *World J Mens Health*. 2018;36(3):192–198. doi:10.5534/wjmh.180001
12. Batsis JA, Villareal DT. Sarcopenic obesity in older adults: aetiology, epidemiology and treatment strategies. *Nat Rev Endocrinol*. 2018;14(9):513–537. doi:10.1038/s41574-018-0062-9
13. Asrih M, Wei S, Nguyen TT, Yi H-S, Ryu D, Gariani K. Overview of growth differentiation factor 15 in metabolic syndrome. *J Cell Mol Med*. 2023;27(9):1157–1167. doi:10.1111/jcmm.17725
14. Jung HW, Park JH, Kim DA, et al. Association between serum FGF21 level and sarcopenia in older adults. *Bone*. 2021;145:115877. doi:10.1016/j.bone.2021.115877
15. Moon JS, Goeminne LJE, Kim JT, et al. Growth differentiation factor 15 protects against the aging-mediated systemic inflammatory response in humans and mice. *Aging Cell*. 2020;19(8):e13195. doi:10.1111/acel.13195
16. Barazzoni R, Bischoff S, Boirie Y, et al. Sarcopenic obesity: time to meet the challenge. *Obes Facts*. 2018;11(4):294–305. doi:10.1159/000490361
17. Takahara T, Amemiya Y, Sugiyama R, Maki M, Shibata H. Amino acid-dependent control of mTORC1 signaling: a variety of regulatory modes. *J Biomed Sci*. 2020;27(1):87. doi:10.1186/s12929-020-00679-2
18. Ruegsegger GN, Creo AL, Cortes TM, Dasari S, Nair KS. Altered mitochondrial function in insulin-deficient and insulin-resistant states. *J Clin Invest*. 2018;128(9):3671–3681. doi:10.1172/JCI120843

19. Dickinson JM, Fry CS, Drummond MJ, et al. Mammalian target of rapamycin complex 1 activation is required for the stimulation of human skeletal muscle protein synthesis by essential amino Acids1–3. *J Nutr*. 2011;141(5):856–862. doi:10.3945/jn.111.139485
20. Dong XC, Copps KD, Guo S, et al. Inactivation of hepatic Foxo1 by insulin signaling is required for adaptive nutrient homeostasis and endocrine growth regulation. *Cell Metab*. 2008;8(1):65–76. doi:10.1016/j.cmet.2008.06.006
21. Sancak Y, Peterson TR, Shaul YD, et al. The Rag GTPases bind raptor and mediate amino acid signaling to mTORC1. *Science*. 2008;320 (5882):1496–1501. doi:10.1126/science.1157535
22. Lecker SH, Goldberg AL, Mitch WE. Protein degradation by the ubiquitin–proteasome pathway in normal and disease states. *J Am Soc Nephrol*. 2006;17(7):1807–1819. doi:10.1681/ASN.2006010083
23. Calnan DR, Brunet A. The FoxO code. *Oncogene*. 2008;27(16):2276–2288. doi:10.1038/onc.2008.21
24. Giresi PG, Stevenson EJ, Theilhaber J, et al. Identification of a molecular signature of sarcopenia. *Physiol Genomics*. 2005;21(2):253–263. doi:10.1152/physiolgenomics.00249.2004
25. Nair S, Lee YH, Rousseau E, et al. Increased expression of inflammation-related genes in cultured preadipocytes/stromal vascular cells from obese compared with non-obese Pima Indians. *Diabetologia*. 2005;48(9):1784–1788. doi:10.1007/s00125-005-1868-2
26. Chen Y, Zhang Z, Hu X, Zhang Y. Epigenetic characterization of sarcopenia-associated genes based on machine learning and network screening. *Eur J Med Res*. 2024;29(1):54. doi:10.1186/s40001-023-01603-8
27. Oort PJ, Knotts TA, Grino M, et al. γ-synuclein is an adipocyte-neuron gene coordinately expressed with leptin and increased in human obesity,3. *J Nutr*. 2008;138(5):841–848. doi:10.1093/jn/138.5.841
28. Lanza IR, Short DK, Short KR, et al. Endurance exercise as a countermeasure for aging. *Diabetes*. 2008;57(11):2933–2942. doi:10.2337/db08-0349
29. Walker JM, Garcet S, Aleman JO, et al. Obesity and ethnicity alter gene expression in skin. *Sci Rep*. 2020;10(1):14079. doi:10.1038/s41598-020-70244-2
30. Langfelder P, Horvath S. WGCNA: an R package for weighted correlation network analysis. *BMC Bioinformatics*. 2008;9(1):559. doi:10.1186/1471-2105-9-559
31. Ritchie ME, Phipson B, Wu D, et al. limma powers differential expression analyses for RNA-sequencing and microarray studies. *Nucleic Acids Res*. 2015;43(7):e47. doi:10.1093/nar/gkv007
32. Zhou Y, Zhou B, Pache L, et al. Metascape provides a biologist-oriented resource for the analysis of systems-level datasets. *Nat Commun*. 2019;10 (1):1523. doi:10.1038/s41467-019-09234-6
33. Szklarczyk D, Gable AL, Nastou KC, et al. The STRING database in 2021: customizable protein–protein networks, and functional characterization of user-uploaded gene/measurement sets. *Nucleic Acids Res*. 2021;49(D1):D605–D612. doi:10.1093/nar/gkaa1074
34. Shannon P, Markiel A, Ozier O, et al. Cytoscape: a software environment for integrated models of biomolecular interaction networks. *Genome Res*. 2003;13(11):2498–2504. doi:10.1101/gr.1239303
35. Lin CY, Chin CH, Wu HH et al. Hubba: hub objects analyzer—a framework of interactome hubs identification for network biology. *Nucleic Acids Res*. 2008;36(suppl_2):W438–443. doi:10.1093/nar/gkn257
36. Becht E, Giraldo NA, Lacroix L, et al. Estimating the population abundance of tissue-infiltrating immune and stromal cell populations using gene expression. *Genome Biol*. 2016;17(1):218. doi:10.1186/s13059-016-1070-5
37. Gu XJ, Su WM, Dou M, et al. Expanding causal genes for Parkinson's disease via multi-omics analysis. *NPJ Parkinsons Dis*. 2023;9(1):146. doi:10.1038/s41531-023-00591-0
38. Burgess S, Thompson SG. CRP CHD genetics collaboration. Avoiding bias from weak instruments in Mendelian randomization studies. *Int J Epidemiol*. 2011;40(3):755–764. doi:10.1093/ije/dyr036
39. Donini LM, Busetto L, Bischoff SC, et al. Definition and diagnostic criteria for sarcopenic obesity: ESPEN and EASO consensus statement. *Obes Facts*. 2022;15(3):321–335. doi:10.1159/000521241
40. YU W, CHEN F, LI N, et al. Sarcopenic obesity in the elderly: etiology, diagnosis, and treatment strategies. *Chin J Geriatr*. 2024;43 (12):1545–1550. doi:10.3760/cma.j.issn.0254-9026.2024.12.006
41. Woo J, Leung J, Morley JE. Validating the SARC-F: a suitable community screening tool for sarcopenia? *J Am Med Dir Assoc*. 2014;15 (9):630–634. doi:10.1016/j.jamda.2014.04.021
42. WHO Expert Consultation. Appropriate body-mass index for Asian populations and its implications for policy and intervention strategies. *Lancet*. 2004;363(9403):157–163. doi:10.1016/S0140-6736(03)15268-3
43. Chen LK, Woo J, Assantachai P, et al. Asian working group for sarcopenia: 2019 consensus update on Sarcopenia diagnosis and treatment. *J Am Med Dir Assoc*. 2020;21(3):300–307.e2. doi:10.1016/j.jamda.2019.12.012
44. Janssen I, Heymsfield SB, Ross R. Low relative skeletal muscle mass (sarcopenia) in older persons is associated with functional impairment and physical disability. *J Am Geriatr Soc*. 2002;50(5):889–896. doi:10.1046/j.1532-5415.2002.50216.x
45. Eknoyan G. Adolphe quetelet (1796 1874) the average man and indices of obesity. *Nephrol Dial Transplant*. 2007;23(1):47–51. doi:10.1093/ndt/gfm517
46. Fried LP, Tangen CM, Walston J, et al. Frailty in older adults: evidence for a phenotype. *J Gerontol a Biol Sci Med Sci*. 2001;56(3):M146–156. doi:10.1093/gerona/56.3.m146
47. Xuekelati S, Maimaitiwusiman Z, Xiang H, Wumaer A, Bai X, Wang H. Handgrip strength: a simple and effective tool to recognize decreased intrinsic capacity in Chinese older adults. *Exp Gerontol*. 2024;196:112567. doi:10.1016/j.exger.2024.112567
48. Hemani G, Zheng J, Elsworth B, et al. The MR-base platform supports systematic causal inference across the human phenome. *Elife*. 2018:7: e34408. doi:10.7554/eLife.34408
49. Burgess S, Butterworth A, Thompson SG. Mendelian randomization analysis with multiple genetic variants using summarized data. *Genet Epidemiol*. 2013;37(7):658–665. doi:10.1002/gepi.21758
50. Bowden J, Davey Smith G, Burgess S. Mendelian randomization with invalid instruments: effect estimation and bias detection through Egger regression. *Int J Epidemiol*. 2015;44(2):512–525. doi:10.1093/ije/dyv080
51. Verbanck M, Chen C-Y, Neale B, Do R. Detection of widespread horizontal pleiotropy in causal relationships inferred from Mendelian randomization between complex traits and diseases. *Nat Genet*. 2018;50(5):693–698. doi:10.1038/s41588-018-0099-7
52. Bowden J, Del Greco MF, Minelli C, et al. Improving the accuracy of two-sample summary-data Mendelian randomization: moving beyond the NOME assumption. *Int J Epidemiol*. 2019;48(3):728–742. doi:10.1093/ije/dyy258

53. Zheng Z, Yuan D, Shen C, Zhang Z, Ye J, Zhu L. Identification of potential diagnostic biomarkers of atherosclerosis based on bioinformatics strategy. *BMC Med Genomics*. 2023;16(1):100. doi:10.1186/s12920-023-01531-w
54. Wu X, Pan J, Pan X, et al. Identification of potential diagnostic biomarkers of carotid atherosclerosis in obese populations. *J Inflamm Res*. 2025;18:1969–1991. doi:10.2147/JIR.S504480
55. Zhang XL, Zhang XF, Fang Y, et al. A possible genetic association between obesity and colon cancer in females. *Front Endocrinol*. 2023;14:1189570. doi:10.3389/fendo.2023.1189570
56. Szöllósi J, Horejsí V, Bene L, Angelisová P, Damjanovich S. Supramolecular complexes of MHC class I, MHC class II, CD20, and tetraspan molecules (CD53, CD81, and CD82) at the surface of a B cell line JY. *J Immunol*. 1996;157(7):2939–2946. doi:10.4049/jimmunol.157.7.2939
57. Dunlock VE. Tetraspanin CD53: an overlooked regulator of immune cell function. *Med Microbiol Immunol*. 2020;209(4):545–552. doi:10.1007/s00430-020-00677-z
58. Meng X, Liu Z, Zhang L, He Y. Plac1 remodels the tumor immune evasion microenvironment and predicts therapeutic response in head and neck squamous cell carcinoma. *Front Oncol*. 2022;12:919436. doi:10.3389/fonc.2022.919436
59. Wen Y, Shang Y, Wang Q. Exploration of the mechanism of linoleic acid metabolism dysregulation in metabolic syndrome. *Genetics Res*. 2022;2022:6793346. doi:10.1038/s41574-018-0062-9
60. Han JH, Jang KW, Myung CS. Garcinia cambogia attenuates adipogenesis by affecting CEBPB and SQSTM1/p62-mediated selective autophagic degradation of KLF3 through RPS6KA1 and STAT3 suppression. *Autophagy*. 2022;18(3):518–539. doi:10.1080/15548627.2021.1936356
61. Zhang JW, Klemm DJ, Vinson C, Lane MD. Role of CREB in transcriptional regulation of CCAAT/enhancer-binding protein β gene during adipogenesis. *J Biol Chem*. 2004;279(6):4471–4478. doi:10.1074/jbc.M311327200
62. Masuda S, Yamakawa K, Masuda A, et al. Association of sarcopenia with a poor prognosis and decreased tumor-infiltrating CD8-positive T cells in pancreatic ductal adenocarcinoma: a retrospective analysis. *Ann Surg Oncol*. 2023;30(9):5776–5787. doi:10.1245/s10434-023-13569-2
63. Zhang X, Zhu G, Zhang F, et al. Identification of a novel immune-related transcriptional regulatory network in sarcopenia. *BMC Geriatr*. 2023;23(1):463. doi:10.1186/s12877-023-04152-1
64. Heo SJ, Jee YS. Characteristics of age classification into five-year intervals to explain sarcopenia and immune cells in older adults. *Medicina*. 2023;59(10):1700. doi:10.3390/medicina59101700
65. Tenuta M, Pandozzi C, Sciarra F, et al. Circulating natural killer cells as prognostic value for non-small-cell lung cancer patients treated with immune checkpoint inhibitors: correlation with sarcopenia. *Cancers*. 2023;15(14):3592. doi:10.3390/cancers15143592
66. Matthews VB, Aström MB, Chan MH, et al. Brain-derived neurotrophic factor is produced by skeletal muscle cells in response to contraction and enhances fat oxidation via activation of AMP-activated protein kinase. *Diabetologia*. 2009;52(7):1409–1418. doi:10.1007/s00125-009-1364-1
67. Just-Borràs L, Hurtado E, Cilleros-Mañé V, et al. Overview of impaired BDNF signaling, their coupled downstream serine-threonine kinases and SNARE/SM complex in the neuromuscular junction of the amyotrophic lateral sclerosis model SOD1-G93A mice. *Mol Neurobiol*. 2019;56(10):6856–6872. doi:10.1007/s12035-019-1550-1
68. Cefis M, Chaney R, Quirié A, et al. Endothelial cells are an important source of BDNF in rat skeletal muscle. *Sci Rep*. 2022;12(1):311. doi:10.1038/s41598-021-03740-8
69. Graupera M, Claret M. Endothelial cells: new players in obesity and related metabolic disorders. *Trends Endocrinol Metab*. 2018;29(11):781–794. doi:10.1016/j.tem.2018.09.003
70. Ginaldi L, De Martinis M, Matutes E, et al. Levels of expression of CD52 in normal and leukemic B and T cells: correlation with in vivo therapeutic responses to Campath-1H. *Leuk Res*. 1998;22(2):185–191. doi:10.1016/s0145-2126(97)00158-6
71. Jiang J, Hiron TK, Agbaedeng TA, et al. A novel macrophage subpopulation conveys increased genetic risk of coronary artery disease. *Circulation Res*. 2024;135(1). doi:10.1161/CIRCRESAHA.123.324172
72. Mao R, Yang F, Zhang Y, et al. High expression of CD52 in adipocytes: a potential therapeutic target for obesity with type 2 diabetes. *Aging*. 2021;13(8). doi:10.18632/aging.202714
73. De Biase D, Piegari G, Prisco F, et al. Implication of the NLRP3 inflammasome in bovine age-related sarcopenia. *Int J Mol Sci*. 2021;22(7):3609. doi:10.3390/ijms22073609
74. Huang SW, Xu T, Zhang CT, Zhou HL. Relationship of peripheral lymphocyte subsets and skeletal muscle mass index in sarcopenia: a cross-sectional study. *J Nutr Health Aging*. 2020;24(3):325–329. doi:10.1007/s12603-020-1329-0
75. Nelke C, Dziewas R, Minnerup J, Meuth SG, Ruck T. Skeletal muscle as potential central link between sarcopenia and immune senescence. *EBioMedicine*. 2019;49:381–388. doi:10.1016/j.ebiom.2019.10.034
76. Saini J, McPhee JS, Al-Dabbagh S et al. Regenerative function of immune system: modulation of muscle stem cells. *Ageing Res Rev*. 2016;27:67–76. doi:10.1016/j.arr.2016.03.006